© Indian Academy of Sciences

**REGULAR ARTICLE**

# Investigation of the efficacy on tyrosinase enzyme of 5-substituted-1H-tetrazole derivatives synthesized with Pd-containing nanoparticle

ELIF AYDINLI[a,b], ZEYAD ADIL HAMEED[c], HAYDAR GOKSU[b,*] and SEVKI ADEM[c]

[a]Department of Natural, Herbal and Cosmetic Products, Institute of Health Sciences, Düzce University, 81620 Düzce, Turkey
[b]Kaynasli Vocational College, Düzce University, 81900 Düzce, Turkey
[c]Department of Chemistry, Faculty of Science, Çankırı Karatekin University, 18100 Çankırı, Turkey
E-mail: haydargoksu@duzce.edu.tr

**Abstract.** Synthesis of 5-substituted-1H-tetrazole derivatives from aryl aldehydes under the influence of Palladium nanoparticles entrapped in aluminum hydroxide matrix (Pd/AlO(OH) NPs) was carried out in ethanol for 3-6 h. The use of the catalyst in this synthesis is the first. Sodium azide and malononitrile used in the reaction are chemical compounds required in the synthesis of tetrazoles. The reactions were concluded with good yields under thermal conditions. In the reactions, twelve derivatives were synthesized. The synthesized compounds were characterized by IR, $^1$H, and $^{13}$C NMR. The olefinic proton's signal, which is around 8.5 ppm, reveals the formation of the tetrazole ring. The tyrosinase enzyme activity for each synthesized derivative was examined, and the results were recorded. According to the results obtained, all tetrazole derivatives were found to be effective compounds for tyrosinase enzyme inhibition. 3-(3,4-dichlorophenyl)-2-(1H-tetrazol-5-yl)acrylonitrile (2k) with two chloride groups at the meta and para position of the phenyl ring seems to be the most potent tyrosinase inhibitor with an $IC_{50}$ value of 45 μM.

**Keywords.** Tetrazole; Tyrosinase; Nanoparticle.

## 1. Introduction

Tetrazole compounds are in the class of heterocyclic compounds containing nitrogen atoms in their structure. Acid and base classifications can be made based on their structures. Tetrazoles are of great interest in fields such as medicinal chemistry, pharmacology, and drug design, especially because of their bioisosteres. Many drugs approved by the FDA (Food and Drug Administration) contain tetrazole parts in their structure.[1] Losartan, valsartan, and cardesartan are the best-known anti-hypertensive drugs (Figure 1).[2]

Molecules modified with tetrazole fragments are resistant to metabolic degradation and chemical oxidants in biological transformations. Therefore, tetrazoles tend to reduce the side effects of drugs by increasing bioavailability and lipophilicity compared to carboxylic acids.[3] The importance of drugs designed in this direction has increased in chemistry, pharmaceuticals, and drug design due to their physicochemical properties, such as absorption, distribution, metabolism, and excretion. Studies of the structure-based design of novel inhibitors on the compatibility and interaction of the tetrazole moiety with receptors have recently shed light on synthetic approaches. Tetrazole fragmented molecules have been evaluated as anti-cancer agents as inhibitors of cyclooxygenase.[4] Intended as a drug candidate for treating hyperuricemia as an inhibitor of xanthine oxidoreductase (XOR) and for treating diabetes as inhibitors of α-amylase and non-enzymatic glycation.[5] Tetrazole and its derivatives have been reported as analgesic, antifungal, anti-inflammatory, antibacterial, antiviral, anti-proliferative agents, potential anti-HIV drug candidates, herbicidal, anti-cancer agents, and multifunctional drug carriers. Besides that tetrazole and its derivatives have been reported as antifungal,[6] anti-inflammatory,[7] antibacterial,[8] antiviral,[9] potential anti-HIV drug candidates,[10] anti-malarial,[11] anticancer,[12] antitümör[13] and
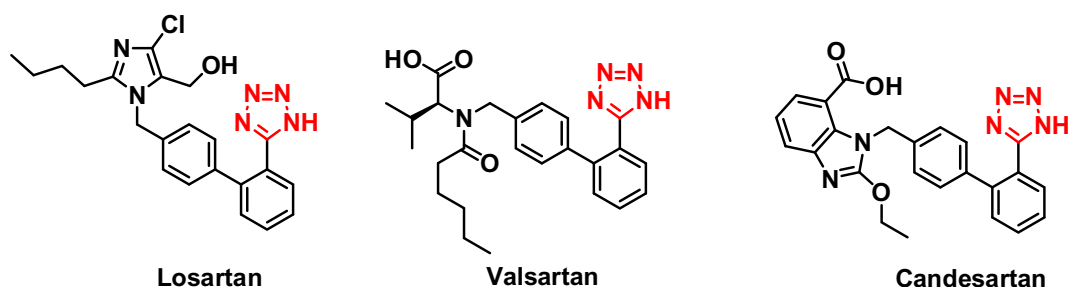
**Figure 1.** Structure of some angiotensin receptor blockers used as drugs containing tetrazole moiety[2]

multifunctional drug carriers agents.[14] Materials science has important applications as a gas generator for airbags in the automobile industry,[15] modern explosives in the defense industry,[16] propellant components for rockets,[17] a photostabilizer and anti-sludging in photography.[18]

Many methods have been reported in the literature for the design of 5-substituted-1H-tetrazoles from various starting materials. The most common method for 5-substituted-1H-tetrazoles is the cycloaddition of azide [3 + 2] to nitriles selected as substrates.[19] Thus, 5-substituted-1H-tetrazole can be synthesized directly. Another method involves a one-pot process of multi-step synthesis, involving 1,3-dipolar cycloaddition and Knoevenagel condensation, of carbonyl determined as substrate. This method is known as Multicomponent domino reactions (MCRs).[20] Known as multicomponent domino reactions (MCRs), this process reduces reaction time, minimizes multi-step reactions and their purification steps, and yields raw materials without complex product isolation. Over the last decade, various catalysts and different solvent systems have been proposed for these processes of 5-substituted-1H-tetrazoles. Homogeneous or heterogeneous catalysts are used in such syntheses.[21] Recently, researchers have been tending to use nanomaterial-based catalysts in their synthesis. Nano-NiO,[20] nano-Fe$_3$O$_4$,[20] nano-Fe$_3$O$_4$/In,[22] nano-ZrP$_2$O$_7$,[23] nano-Cu-MOF[19] are examples of nanoparticle-based catalysts. Catalysts which modified with different materials formed with boehmit nanoparticles (BNPs) (BNPs@SiO$_2$-TPPTSA,[21a] Ni-SMTU@boehmite,[19] Fe$_3$O$_4$@BNPs-CPTMS-Chitosan-Pd(0),[21] magnetic carbon nanotubes (Fe$_3$O$_4$-CNT-SO$_3$H),[24] magnetic nano-biocomposites (Fe$_3$O$_4$@ fibroin-SO$_3$H),[25] magnetic nanoparticles (MNPs) (NH–Cu(II)@MNP),[26] mesoporous organosilica (nano-Fe$_3$O$_4$@PMO-ICS-ZnO)[27] have been reported for the synthesis of 5-substituted-1H-tetrazoles. The syntheses were carried out under various environmental conditions such as ultrasonication, microwave, solvent-free conditions, water, magnetized water, methanol, ethanol, DMF, PEG, and Ionic liquids.
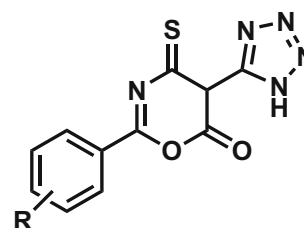


**Figure 2.** Tetrazole derivative, which is a tyrosinase inhibitor

The presence of four nitrogen atoms that can form coordination bonds in the tetrazole ring enables the use of tetrazoles as ligands and to obtain various metal complexes. The chelating ability can cause them to exert an inhibitory effect in a way that reduces the efficiency of the enzyme in coordination with metalloenzymes. Tyrosinase is a multifunctional metalloenzyme with two copper ions coordinated to three different amino acids at its active center. Tyrosinase inhibitors also cause inhibition by enzyme-substrate interaction by chelating with the copper metal ion in the tyrosinase enzyme, or they function by inhibiting the oxidation process involved in the formation of melanin.

In studies for molecules containing tetrazole fragments, mostly molecular docking modeling studies were carried out during the design process of tyrosinase inhibitors. The probability of 5-substituted-1H-tetrazole derivatives being chelators of copper atoms was predicted by molecular docking calculations. In this context, Joonhyeok Choi and colleagues identified carboxylic acid, thiol/thione, triazole, as well as tetrazole groups as novel binding nuclei that interact with the dicopper catalytic center of the tyrosine enzyme by structure-based virtual scanning (SBVS).[28]

However, very few studies have gone a step further and investigated their inhibitory potential against fungal tyrosinase *in vitro*. Rabia Qamar *et al.,* demonstrated by molecular docking analysis that tetrazole hybrids exhibit a valid tyrosinase inhibitory activity against melanogenesis, and their inhibitory

potential against fungal tyrosinase was confirmed by *in vitro* studies (Figure 2).[29]

## 2. Experimental

### 2.1 *Chemistry*

All of the aryl aldehydes, palladium nanoparticles entrapped in aluminum hydroxide matrix (Pd/AlO(OH) NPs), malononitrile $(CH_2(CN)_2)$, sodiumazide $(NaN_3)$ used in the study were obtained from Sigma-Aldrich and Merck companies. Solvents such as ethyl alcohol, *n*-hexane, ethyl acetate, dichloromethane, and methyl alcohol used in the experimental process were obtained from Sigma-Aldrich and were not subjected to any treatment. Enzyme and its substrate were procured from Sigma-Aldrich.

2.1a *Characterization methods*: ^{1}H NMR and ^{13}C NMR spectra were recorded with the Bruker AVANCE III 400 MHz NMR Spectrometer. The melting point determinations were recorded with Stuart Automatic Melting Point. FTIR spectra were recorded with the cary 630 FTIR Attenuated Total Reflection (ATR).

2.1b *General procedure for the synthesis of tetrazole compounds*: Aryl aldehyde derivatives (1.0 mmol), malononitrile (1.1 mmol), sodium azide (1.2 mmol), and 0.03 g of Pd/AlO(OH) NPs catalyst were mixed in 10 mL of ethanol in a single neck flask. The reactions were continued for 3-6 h under reflux. The reaction was controlled by thin layer chromatography (TLC) $(SiO_2$, hexane:ethyl acetate (EtOAc)=4:1 (v/v)). After the reaction was completed, the catalyst was removed by a simple centrifugation. The remaining filtrate was added to 30 mL of 2 N HCl solution and stirred vigorously for 30 min. The mixture was worked up twice with the help of ethyl acetate. After the organic phases were combined, the solvent was removed. A simple resolution technique purified the remaining solid without the need for column chromatography. IR, ^{1}H NMR, and ^{13}C NMR spectra identified the structures of the respective tetrazole derivatives.

2.1.1a. *3-phenyl-2-(1H-tetrazol-5-yl)acrylonitrile (2a):* ^{1}H NMR (400 MHz, DMSO-d$_6$) δ 8.40 (s, 1H, C=C*H*), 8.10–7.96 (m, 2H, Ar*H*), 7.68–7.48 (m, 3H, Ar*H*). ^{13}C NMR (100 MHz, DMSO-d$_6$) δ 155.95, 148.86, 132.80, 132.63, 130.32, 129.78, 115.99, 97.42.
FT-IR(cm$^{-1}$): 3591.9, 3186.1, 2223.3, 1563.5, 1451.2, 1370.4, 1294.6, 1213.7

2.1.1b. *3-(4-hydroxyphenyl)-2-(1H-tetrazol-5-yl)acrylonitrile (2b)* ^{1}H NMR (400 MHz, DMSO-d$_6$) δ 10.64 (bs, 1H, O*H*), 8.21 (s, 1H, C=C*H*), 7.94 (d, *J* = 8.8 Hz, 2H, Ar*H*), 6.97 (d, *J* = 8.7 Hz, 2H, Ar*H*). ^{13}C NMR (100 MHz, DMSO-d$_6$) δ 162.12, 148.42, 133.03, 123.84, 116.82, 116.77, 92.36.
FT-IR(cm$^{-1}$): 3385.9, 3107.5, 2222.3, 1559.7, 1437.1, 1364.8, 1288.7

2.1.1c. *3-(2,5-dihydroxyphenyl)-2-(1H-tetrazol-5-yl)-acrylonitrile (2c)* ^{1}H NMR (400 MHz, DMSO-d$_6$) δ 10.09 (s, 1H, ArO*H*), 8.88 (s, 1H, C=C*H*), 7.37 (d, *J* = 9.0 Hz, 1H, Ar*H*), 7.22 (dd, *J* = 9.0, 2.9 Hz, 1H, Ar*H*), 7.11 (d, *J* = 2.9 Hz, 1H, Ar*H*). ^{13}C NMR (100 MHz, DMSO-d$_6$) δ 157.60, 154.84, 153.88, 147.92, 124.04, 118.44, 118.29, 115.24, 113.80, 102.47.
FT-IR(cm$^{-1}$): 3318.6, 3124.2, 2237.9, 1565.7, 1482.5, 1299.0, 1265.1

2.1.1d. *3-(2,5-dimethoxyphenyl)-2-(1H-tetrazol-5-yl)-acrylonitrile (2d)* ^{1}H NMR (400 MHz, DMSO-d$_6$) δ 8.53 (s, 1H, C=C*H*), 7.72 (d, *J* = 2.7 Hz, 1H, Ar*H*), 7.23-7.12 (m, 2H, Ar*H*), 3.87 (s, 3H, OC*H$_3$*), 3.78 (s, 3H, OC*H$_3$*). ^{13}C NMR (100 MHz, DMSO-d$_6$) δ 155.92, 153.20, 153.16, 142.80, 121.39, 120.40, 116.06, 113.68, 113.00, 97.44, 56.80, 56.02.
FT-IR(cm$^{-1}$): 3492.7, 3114.1, 2930.4, 2227.2, 1589.1, 1497.1, 1465.7, 1224.3, 1028.4

2.1.1e. *3-(3,4-dimethoxyphenyl)-2-(1H-tetrazol-5-yl)-acrylonitrile (2e)* ^{1}H NMR (400 MHz, DMSO-d$_6$) δ 8.29 (s, 1H, C=C*H*), 7.75 (s, 1H, Ar*H*), 7.65 (d, *J* = 8.4 Hz, 1H, Ar*H*), 7.19 (d, *J* = 8.5 Hz, 1H, Ar*H*), 3.88 (s, 3H, OC*H$_3$*), 3.84 (s, 3H, OC*H$_3$*). ^{13}C NMR (100 MHz, DMSO-d$_6$) δ 155.93, 152.98, 149.18, 148.76, 125.86, 125.25, 116.69, 112.34, 93.40, 56.28, 55.93.
FT-IR(cm$^{-1}$): 3180.7, 2210.8, 1584.4, 1513.2, 1447.3, 1340.6, 1245.2, 1140.0

2.1.1f. *2-(1H-tetrazol-5-yl)-3-(3,4,5-trimethoxyphenyl)-acrylonitrile (2f)* ^{1}H NMR (400 MHz, DMSO-d$_6$) δ 8.34 (s, 1H, C=C*H*), 7.45 (s, 2H, Ar*H*), 3.86 (s, 6H, OC*H$_3$*), 3.78 (s, 3H, OC*H$_3$*). ^{13}C NMR (100 MHz, DMSO-d$_6$) δ 153.42, 148.58, 141.40, 127.93, 116.54, 108.91, 108.13, 96.32, 60.78, 56.48.
FT-IR(cm$^{-1}$): 3412.6, 3089.0, 2933.6, 2214.6, 1578.8, 1508.7, 1452.2, 1331.7, 1129.5

2.1.1g. *2-(1H-tetrazol-5-yl)-3-o-tolylacrylonitrile (2g):* ^{1}H NMR (400 MHz, DMSO-d$_6$) δ 8.53 (s, 1H, C=C*H*), 7.97 (d, *J* = 7.4 Hz, 1H, Ar*H*), 7.52-7.36 (m, 3H, Ar*H*), 2.43 (s, 3H, C*H$_3$*). ^{13}C NMR (100 MHz,

DMSO-d$_6$) $\delta$ 155.32, 147.74, 139.19, 132.13, 131.97, 131.27, 128.27, 126.83, 115.77, 99.63, 19.86.

FT-IR(cm$^{-1}$): 3390.2, 3170.1, 3092.8, 2217.4, 1599.0, 1451.1, 1373.9, 1281.4, 1223.9, 1025.2

*2.1.1h. 2-(1H-tetrazol-5-yl)-3-p-tolylacrylonitrile (2h):* $^1$H NMR (400 MHz, DMSO-d$_6$) $\delta$ 8.33 (s, 1H, C=C*H*), 7.93 (d, *J* = 8.1 Hz, 2H, Ar*H*), 7.42 (d, *J* = 8.1 Hz, 2H, Ar*H*), 2.41 (s, 3H, C*H$_3$*). $^{13}$C NMR (100 MHz, DMSO-d$_6$) $\delta$ 155.92, 148.54, 143.42, 130.40, 130.01, 116.26, 96.19, 21.73.

FT-IR(cm$^{-1}$): 3407.8, 3206.8, 3175.3, 2218.2, 1594.3, 1422.6, 1184.9

*2.1.1i. 3-(2-fluorophenyl)-2-(1H-tetrazol-5-yl)acry-lonitrile (2i):* $^1$H NMR (400 MHz, DMSO-d$_6$) $\delta$ 8.44 (s, 1H, C=C*H*), 8.22 (m, 1H, Ar*H*), 7.69 (m, 1H, Ar*H*), 7.51-7.40 (m, 2H, Ar*H*). $^{13}$C NMR (100 MHz, DMSO-d$_6$) $\delta$ 162.46, 159.52, 140.07, 134.94, 129.19, 125.69, 120.67, 116.89, 115.42, 100.53.

FT-IR(cm$^{-1}$): 3386.1, 2994.1, 1600.6, 1288.4, 1025.2

*2.1.1j. 3-(4-fluorophenyl)-2-(1H-tetrazol-5-yl)acry-lonitrile (2j):* $^1$H NMR (400 MHz, DMSO-d$_6$) $\delta$ 8.41 (s, 1H, C=C*H*), 8.20-7.99 (m, 2H, Ar*H*), 7.53-7.39 (m, 2H, Ar*H*). $^{13}$C NMR (100 MHz, DMSO-d$_6$) $\delta$ 165.70, 163.19, 147.44, 133.10, 133.00, 129.39, 129.36, 117.14, 116.92, 116.02, 97.25.

FT-IR(cm$^{-1}$): 3377.6, 3184.7, 3109.4, 2204.1, 1586.7, 1507.3, 1232.3, 1160.9

*2.1.1k. 3-(3,4-dichlorophenyl)-2-(1H-tetrazol-5-yl)-acrylonitrile (2k):* $^1$H NMR (400 MHz, DMSO-d$_6$) $\delta$ 8.42 (s, 1H, C=C*H*), 8.27 (s, 1H, Ar*H*), 8.03 (d, *J* = 8.3 Hz, 1H, Ar*H*), 7.90 (d, *J* = 8.5 Hz, 1H, Ar*H*). $^{13}$C NMR (100 MHz, DMSO-d$_6$) $\delta$ 145.45, 134.85, 133.37, 132.42, 132.02, 131.94, 129.84, 118.96, 116.25, 115.70, 100.15.

FT-IR(cm$^{-1}$): 3442.5, 3183.9, 3078.4, 2176.3, 1610.6, 1580.9, 1466.7, 1397.2, 1210.5, 1027.3

*2.1.1l. 3-(5-bromo-2-methoxyphenyl)-2-(1H-tetrazol-5-yl)acrylonitrile (2l):* $^1$H NMR (400 MHz, DMSO-d$_6$) $\delta$ 8.46 (s, 1H, C=C*H*), 8.22 (d, *J* = 2.3 Hz, 1H, Ar*H*), 7.77 (dd, *J* = 8.9, 2.4 Hz 1H, Ar*H*), 7.21 (d, *J* = 9.0 Hz, 1H, Ar*H*), 3.92 (s, 3H, OC*H$_3$*). $^{13}$C NMR (100 MHz, DMSO-d$_6$) $\delta$ 157.84, 141.33, 136.52, 130.83, 123.35, 115.66, 114.88, 112.43, 99.55, 56.90.

FT-IR(cm$^{-1}$): 3414.6, 3114.4, 3114.4, 2981.8, 2216.1, 1608.1, 1585.9, 1477.0, 1251.0, 1178.9, 1004.2

## 2.2 Biochemistry assays

2.2a *In vitro Tyrosinase inhibitory activity*: Tyrosinase inhibitory activity was measured using the mushroom tyrosinase enzyme at 492 nm using a microtiter plate reader, as previously reported.[30] The reaction media (250 mL) for enzyme activity assay contained 0.5 mM L-DOPA in 50 mM phosphate buffer (PH 6.8) and 100 mL of different concentrations of compounds. The reaction was performed at 37 °C over a 7 min period. The compounds were dissolved in 1 mg/mL DMSO and diluted to the proper concentration. The controls without inhibitors but including DMSO in the reaction media were always performed. The inhibitory influences of compounds on the tyrosinase activity were expressed as the concentrations that inhibited 50% of the enzyme activity (IC$_{50}$).

2.2b *Molecular docking*: To acquire a comprehension of the probable binding poses of the synthesized compounds with the tyrosinase active site, a molecular docking study was carried out using the Molegro Virtual Docker program.[31] The X-ray crystal structure of tyrosinase from Agaricus bisporus cocrystallized with tropolone was obtained from RCSB Protein Data Bank (2Y9X).[32] The three-dimensional (3D) structures of compounds **2c** and **2k** were constructed using MarvinSketch. The protein was imported into Molegro Virtual Docker, and the crystal structure was prepared for docking by removing water and optimizing missing amino acids. The binding site for small molecules was described by choosing tropolone as a reference ligand, to which all coordinates were calculated. Ten docking trials were performed for each molecule, and the conformations with the best scores were selected to examine the interaction details in the Discovery Studio 2021 Client.

2.2c *Prediction of ADME Properties*: For the estimation of physicochemical properties, pharmacokinetics, drug-likeness, and medicinal chemistry friendliness of new compounds, we have evaluated the ADME properties using SwisADME online tool.[33]

## 3. Results and Discussion

### 3.1 Chemistry

2,5-dimethoxybenzaldehyde was preferred for optimization studies in the synthesis of 5-substituted-1H-
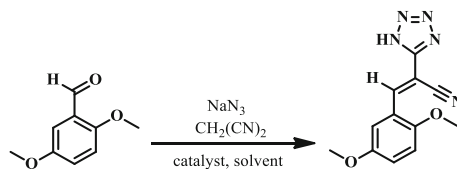
tetrazole derivatives. The effects of PdAlO(OH) nanoparticles on the selected compound were investigated. When the XRD images in our group's previous studies and literature data are examined, it is seen that the catalyst has a Boehmite structure.[34] The standardization of the method was carried out over different temperatures, solvents, and catalyst amounts. Initial trials were carried out with an apolar solvent. However, no product formation was observed due to the reaction (Table 1, entry 1). The reactions of methylene chloride, water, methanol, and ethanol as polar solvents at room temperature were also negative (Table 1, entries 2, 3, 5, 6). However, product formation was observed with increased water temperature, albeit with a low yield (Table 1, entry 4). The inability to obtain the desired efficiency in water and the need for high temperatures led us to ethanol. Therefore, the maximum yield was obtained from the reaction at the boiling temperature of ethanol (Table 1, entry 7). A decrease in reaction efficiency is observed when the amount of catalyst is decreased (Table 1, entry 9). The reaction occurs without a catalyst, but a very low yield is obtained (Table 1, entry 10). In the end, 0.1 mmol substrate, 30 mg catalyst gave sufficient performance to convert 2,5-dimethoxybenzaldehyde to 3-(2,5-dimethoxyphenyl)-2-(1H-tetrazol-5-yl)acrylonitrile with only 5.0 mL of ethanol (Table 1, entry 8).

Aryl aldehyde derivatives were used as starting material for the synthesis of 5-substituted-1H-tetrazole derivatives. This study synthesized tetrazole derivatives from aryl aldehydes in one step. Aryl aldehyde derivatives are converted to tetrazole derivatives through benzylidene malononitrile compounds. For this purpose, it has been determined that the temperature is an important parameter so that the reaction does not remain in the intermediate stage. It was observed that the reaction did not convert to tetrazole derivatives at low temperatures and remained in the benzylidene malononitrile stage. In addition, the solvent environment also affects the course of the reaction. Reactions are completed with better yields in solvents such as methanol and ethanol with high polarity where solubility is strong. A polar solvent such as water was also used in the reactions. However, the expectation ended in disappointment. The most important parameter affecting the reaction efficiency is the catalyst used. Because when the catalyst is not used, the reaction takes place, but both the reaction time is prolonged, and the yield is considerably reduced.

Table 2 shows that a series of aryl aldehydes were converted to 5-substituted-1H-tetrazole under the

**Table 1.** Optimization conditions for synthesizing 3-(2,5-dimethoxyphenyl)-2-(1H-tetrazol-5-yl)acrylonitrile[a]



| Entry | Solvent | Catalyst ($mg$) | Temperature ($^oC$) | Time ($h$) | Yield[b] ($\%$) |
|---|---|---|---|---|---|
| 1 | Toluene | 30 | 110 | 6 | Trace |
| 2 | $CH_2Cl_2$ | 30 | 25 | 6 | Trace |
| 3 | $H_2O$ | 30 | 25 | 6 | Trace |
| 4 | $H_2O$ | 30 | 100 | 6 | 12 |
| 5 | MeOH | 30 | 25 | 6 | Trace |
| 6 | EtOH | 30 | 25 | 6 | Trace |
| 7 | EtOH | 30 | 78 | 6 | 73 |
| **8** | **EtOH** | **30** | **78** | **4** | **73** |
| 9 | EtOH | 10 | 78 | 6 | <50 |
| 10 | EtOH | - | 78 | 6 | ∼40 |

[a]Reaction conditions: Substrate (0.1 mmol), malononitrile (0.11 mmol), sodium azide (0.12 mmol)

[b]NMR yield.

**Table 2.**   Synthesis of 5-substituted-1H-tetrazole derivatives catalyzed by Pd/AlO(OH) NPs (1)[a].



| Entry | Substrate | Product | Time, (hour) | Yield[b] (%) | Mp. (°C) | Entry | Substrate | Product | Time, (hour) | Yield[b] (%) | Mp. (°C) |
|---|---|---|---|---|---|---|---|---|---|---|---|
| 1 | 1a | 2a | 5 | 95 | 168-170 | 7 | 1g | 2g | 4 | 85 | 127-129 |
| 2 | 1b | 2b | 5 | 95 | 175-179 | 8 | 1h | 2h | 4 | 73 | 150-152 |
| 3 | 1c | 2c | 3 | 79 | - | 9 | 1i | 2i | 3 | 95 | 144-147 |
| 4 | 1d | 2d | 4 | 73 | 177-179 | 10 | 1j | 2j | 4 | 95 | 176-179 |
| 5 | 1e | 2e | 5.5 | 79 | 220-222 | 11 | 1k | 2k | 3 | 72 | 134-136 |
| 6 | 1f | 2f | 4 | 85 | 212-214 | 12 | 1l | 2l | 5 | 60 | 220-222 |

[a]Reaction conditions: Substrate (0.1 mmol), malononitrile (0.11 mmol), sodium azide (0.12 mmol), Pd/AlO(OH) NPs catalyst (0.03 g, w/w 0.5% Pd), 5 mL of ethanol.

[b]NMR yield.

effect of a heterogeneous catalyst in good yields in ethanol. Pd/AlO(OH) NPs were used as the heterogeneous catalyst. For example, benzaldehyde (1a) and 4-hydroxy benzaldehyde (1b) were converted to 3-phenyl-2-(1H-tetrazol-5-yl)acrylonitrile (2a) and 3-(4-hydroxyphenyl)-2-(1H-tetrazol-5-yl)acrylonitrile (2b) with 95% yield within 5 h (Table 2, entries 1, 2). 2,5-dihydroxybenzaldehyde (1c) was converted to 3-(2,5-dihydroxyphenyl)-2-(1H-tetrazol-5-yl)acrylonitrile (2c) with 79% yield within 3 h (Table 2, entry 3). 2,5-dimethoxybenzaldehyde (1d) was converted to 3-(2,5-dimethoxyphenyl)-2-(1H-tetrazol-5-yl)acrylonitrile (2d) with 73% yield within 4 h (Table 2, entry 4). 3,4-dimethoxybenzaldehyde (1e) was converted to 3-(3,4-dimethoxyphenyl)-2-(1H-tetrazol-5-yl)acrylonitrile (2e) with 79% yield within 5.5 h (Table 2, entry 5). 3,4,5-trimethoxybenzaldehyde (1f) and 2-methylbenzaldehyde (1g) were converted to 2-(1H-tetrazol-5-yl)-3-(3,4,5-trimethoxyphenyl)acrylonitrile (2f) and 2-(1H-tetrazol-5-yl)-3-o-tolylacrylonitrile (2g) with 85% yield within 4 h (Table 2, enties 6, 7). 2-(1H-tetrazol-5-yl)-3-p-tolylacrylonitrile (2h) was obtained with a 73% yield within 4 h (Table 2, entry 8). 3-(2-fluorophenyl)-2-(1H-tetrazol-5-yl)acrylonitrile (2i) and 3-(4-fluorophenyl)-2-(1H-tetrazol-5-yl)acrylonitrile (2j) were obtained with 95% yield (Table 2, entries 9, 10). 3,4-dichlorobenzaldehyde (1k) was converted to 3-(3,4-dichlorophenyl)-2-(1H-tetrazol-5-yl)acrylonitrile (2k) with 72% yield within 3 h (Table 2, entry 11). 5-bromo-2-methoxybenzaldehyde (1l) was converted to 3-(5-bromo-2-methoxyphenyl)-2-(1H-tetrazol-5-yl)acrylonitrile (2l) with 60% yield within 5 h (Table 2, entry 12).

### 3.2 Biochemistry (Tyrosinase inhibition)

The inhibitory potential of twelve compounds against tyrosinase enzyme activity was tested (Table 3). Compound 2k with two chloride groups at the meta and para position of the phenyl ring seems to be the most potent tyrosinase inhibitor with an IC$_{50}$ value of 45 μM, followed by derivative 2c with two hydroxyl substitutes at the 2- and 5-positions of the phenyl ring (IC$_{50}$= 99 μM). The IC$_{50}$ of the reference molecule tropolone has been reported as 40 μM.[35] *In vitro* study results demonstrated that Compound 2k has reference molecular equivalent inhibition potential.

Compounds 2j, 2b, 2h, 2a, and 2d showed inhibitor effects on enzyme activity with IC$_{50}$ values 173.29, 288.81, 346.57, 433.22, and 577.62 μM, respectively. Tyrosinase was inhibited by 2e, 2f, and 2g with IC$_{50}$ values 693.14, 653.52, and 624.45 μM, respectively.

**Table 3.** Tyrosinase enzyme inhibition values of 5-substituted-1H-tetrazole derivatives.

| Compounds | IC$_{50}$ Value (μM) |
|---|---|
| 2a | 433.2 |
| 2b | 288.8 |
| 2c | 99.0 |
| 2d | 577.6 |
| 2e | 693.1 |
| 2f | 653.5 |
| 2g | 624.4 |
| 2h | 346.6 |
| 2i | – |
| 2j | 173.3 |
| **2k** | **45.0** |
| 2l | – |
| Tropolone* | 40.0 |

*Tropolone was used as a standard inhibitor for the tyrosinase enzyme investigated here.[32]

New molecules are derived by adding different substituents on the phenyl ring at different positions. When we compare the results with the first molecules without any group attached, it can be said that the groups attached to the para position significantly contribute to the inhibition effect of molecules against the enzyme. While the inhibition potential of 2j and 2h molecules with fluorine and methyl groups in the para position increased, the inhibition potential of molecule 2g with methyl in the ortho position decreased, and molecule 2i with fluorine did not show any inhibition effect. As seen in compounds 2d, 2e, and 2f, methoxy substituents reduced the inhibition potential of the molecule against the enzyme. This may be due to the fact that the molecule cannot get close enough to the active site due to cystic hindrance. As seen in compounds 2d, 2e, and 2f, functional group methoxy substituents reduced the inhibition potential of the molecule against the enzyme. This may be because the molecule cannot get close enough to the active site due to steric hindrance. When the activities of the 2c and 2d molecules with -OH and -OCH$_3$ in the same positions are compared, the inhibition potential of the molecule 2c with -OH has increased, whereas the inhibition potential of the molecule 2d with -OCH$_3$ has decreased. A similar activity change was also observed in molecules 2e and 2k. The results ensure a comprehensive investigation into the important role of the substitution structure on the phenyl group present at the 5-substituted-1H-tetrazole terminal for developing potent tyrosinase inhibitors.

3.2a *Molecular docking*:   The docking studies for the synthesized compounds 2c and 2k were carried out to evaluate the binding and orientations of ligands against Tyrosinase (2Y9X). The docking was performed using Molegro Virtual Docker, and the docking was confirmed by superimposing the co-crystallized ligand to the docked ligand with RMSD less than 2 Å. A comparison of software-predicted binding geometries with reference ligand, the locations of new derivatives at the active site, and the docking cavity for the enzyme are visualized in Figure 3. Copper ions in the catalytic region make an important contribution to tyrosinase enzyme activity. Their stability is provided by His residues. As seen in Figure 3, Compounds 2c and 2k interact in the same region of the enzyme as the reference ligand that binds near the binuclear copper site.

In Table 4, the docking results of the molecules, the amino acids with which they interact the most, and their energy scores are given. Asn260, His263, and Val283 amino acids are the first three residues with which tropolone and the two tested molecules interact most. Also, this table is visualized in Figure 4 as a network using Cytoscape software.[36] Both compounds could be located in the pocket to which the reference ligand binds by binding to similar amino acids. According to Figure 4, it shows that both molecules interact with all the amino acids with which the reference molecule interacts.[37]
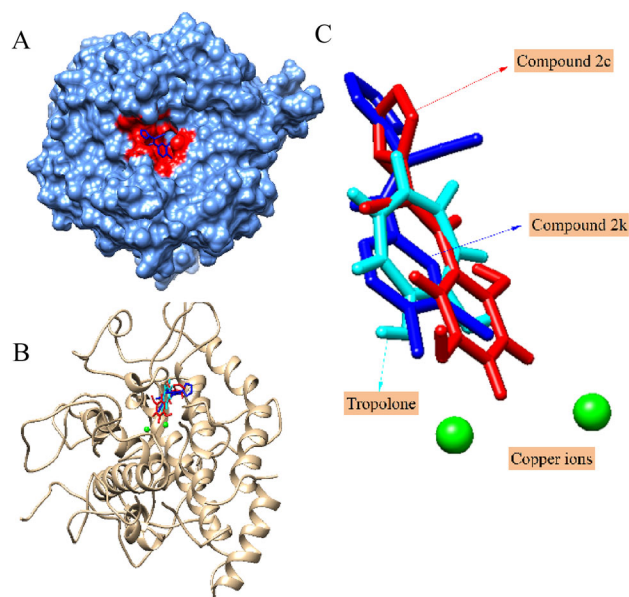


**Figure 3.** The binding domain of compounds towards tyrosinase active site (a) Docking region was shown red color (b) Molecules in the active cavity of the enzyme (c) The overlapping states of compounds 2c and 2k with reference ligand

The docking studies about compounds 2k and 2c into the active cavity of the tyrosinase indicated that several molecular interactions supported the remarkable affinity of these derivatives. In Figure 5, the favorable interactions of the molecules with the active site of tyrosinase are illustrated with 3D and 2D diagrams. Van der Waals interactions, which ensure the stability of molecules in the active site, are also shown in Figure 5.[38]

Derivative 2k is the most active compound against the target in the synthesized library, and its docking score was found to be -99.7873 MolDock Score. It forms the hydrophobic interactions with His259, His263, His61, His85, Val283, and Val248. Chlorines of the benzene ring contributed to Alkyl interactions with His259, His263, His61, His85, and Val285 amino acids. Its interaction revealed that the tetrazole and phenyl rings displayed two π-sigma interactions with the methyl group of Val248 and Val283, respectively. Phenyl ring formed a Pi-Pi Stacked interaction with His263. It formed van der Waals interaction with Phe292, Ser282, Met280, Gly281, Phe264, Asn260, His244 and Met257 (Figure 5).

The binding pose of derivative 2c (docking score -86.5808 MolDock Score) at the tyrosinase binding site revealed that a hydrogen bond interaction was observed between the backbone oxygen of Asn260 and the 2-hydroxyl-substituted at 2-position of the phenyl ring. In addition, the phenyl ring was involved in π-sigma interaction with Val283, in Pi-Pi Stacked interaction with His263, and pi-Alkyl with Ala286. The tetrazole ring interacts with the phenyl group of Phe264 to form a Pi-Pi Stacked interaction. It also showed the van der Waals interaction with residue Phe292, His61, Ser282, Gly281, Val248, His259, Phe90, Glu256, and His244.

It is assumed that the hydrophobic interaction between the copper ion and His263 plays a vital role in the orientation of the substrate.[39] *In silico* images predicted that the benzene ring of the molecules may exhibit a strong Pi-Pi Stached interaction with the imidazole side chain of this amino acid, as in the reference molecule. An interaction similar to that of the reference molecule is seen between the amino acid Val283 and the same benzene ring. These interactions may have contributed to the correct orientation of molecules in the active site for their inhibitory effects. Cu ions, whose stability is provided by Histidine residues, play an important role in the enzyme activity.[32] It is predicted that compound 2c, such as 263, 61, 259, and compound 2k, such as 61, 263, 259, may interact with histidine residues that provide the stability of copper ions. It can be said that these

**Table 4.** Amino acid residues that the most interact with compounds 2k, 2c, and tropolone.

| Compound 2k | | | Compound 2c | | | References ligand (tropolone) | | |
|---|---|---|---|---|---|---|---|---|
| -99.7873 MolDock Score | | | -86.5808 MolDock Score | | | -47.639 MolDock Score | | |
| Residue | ID | Total | Residue | ID | Total | Residue | ID | Total |
| **Asn** | **260** | **-17.49** | **Val** | **283** | **-17.80** | **Val** | **283** | **-13.24** |
| **His** | **263** | **-17.14** | **Asn** | **260** | **-15.84** | **His** | **263** | **-10.45** |
| **Val** | **283** | **-15.15** | **His** | **263** | **-13.04** | **Asn** | **260** | **-5.87** |
| Phe | 264 | -13.67 | Phe | 264 | -10.83 | Ser | 282 | -5.39 |
| Ser | 282 | -6.27 | His | 85 | -6.89 | Phe | 264 | -5.34 |
| Gly | 281 | -4.70 | His | 259 | -5.04 | Gly | 281 | -3.72 |
| Met | 280 | -3.45 | **Ser** | 282 | -5.02 | His | 259 | -2.10 |
| His | 244 | -3.23 | His | 61 | -3.95 | Met | 280 | -2.09 |
| Val | 248 | -3.23 | Phe | 292 | -2.13 | His | 85 | -1.74 |
| His | 259 | -2.56 | Gly | 281 | -2.03 | Cu | 1 | -1.38 |
| His | 61 | -2.40 | Glu | 256 | -1.87 | Ala | 286 | -1.13 |
| Met | 257 | -2.25 | Val | 248 | -1.57 | His | 61 | -0.90 |
| His | 85 | -2.08 | Phe | 90 | -1.25 | | | |
| Cu | 1 | -1.56 | Met | 280 | -1.06 | | | |
| His | 279 | -0.54 | His | 296 | -0.84 | | | |
| Phe | 292 | -0.50 | His | 244 | -0.55 | | | |
| Ala | 286 | 2.81 | Cu | 1 | 1.11 | | | |
| | | | Arg | 268 | 2.00 | | | |
| | | | Ala | 286 | 2.96 | | | |
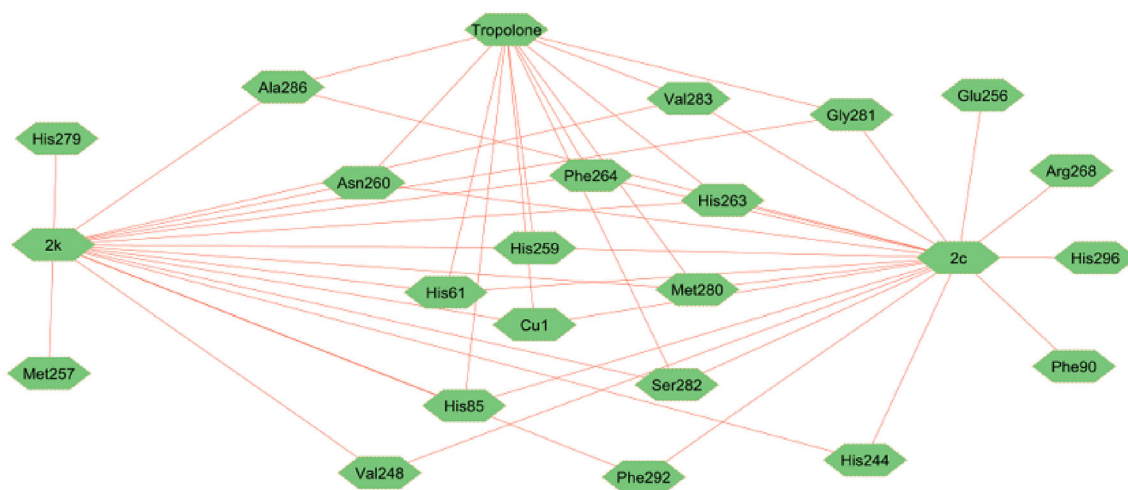


**Figure 4.** Diagram showing which amino acids at the active region of the enzyme interact with the reference molecule and the active molecules

interactions contribute to the inhibitory effect of the molecules.[40]

*In silico* ADME properties of compounds 2c and 2k were predicted using the SwissADME web tool. ADME properties were added to the reference molecule for comparison purposes. The results obtained are presented in Table 5. The BOILED-Egg is a graph that works by calculating the polarity and lipophilicity properties of small molecules and shows their brain and intestinal absorption (Figure 6).[41]

The white zone is for the high expectation of passive transport by gastrointestinal absorption, and the yellow zone (yolk) is for the high possibility of blood-brain barrier penetration. While small intestinal absorption (HIA) of these molecules is quite high, it is estimated that they cannot pass the blood-brain barrier (BBB) passively except for reference molecules.
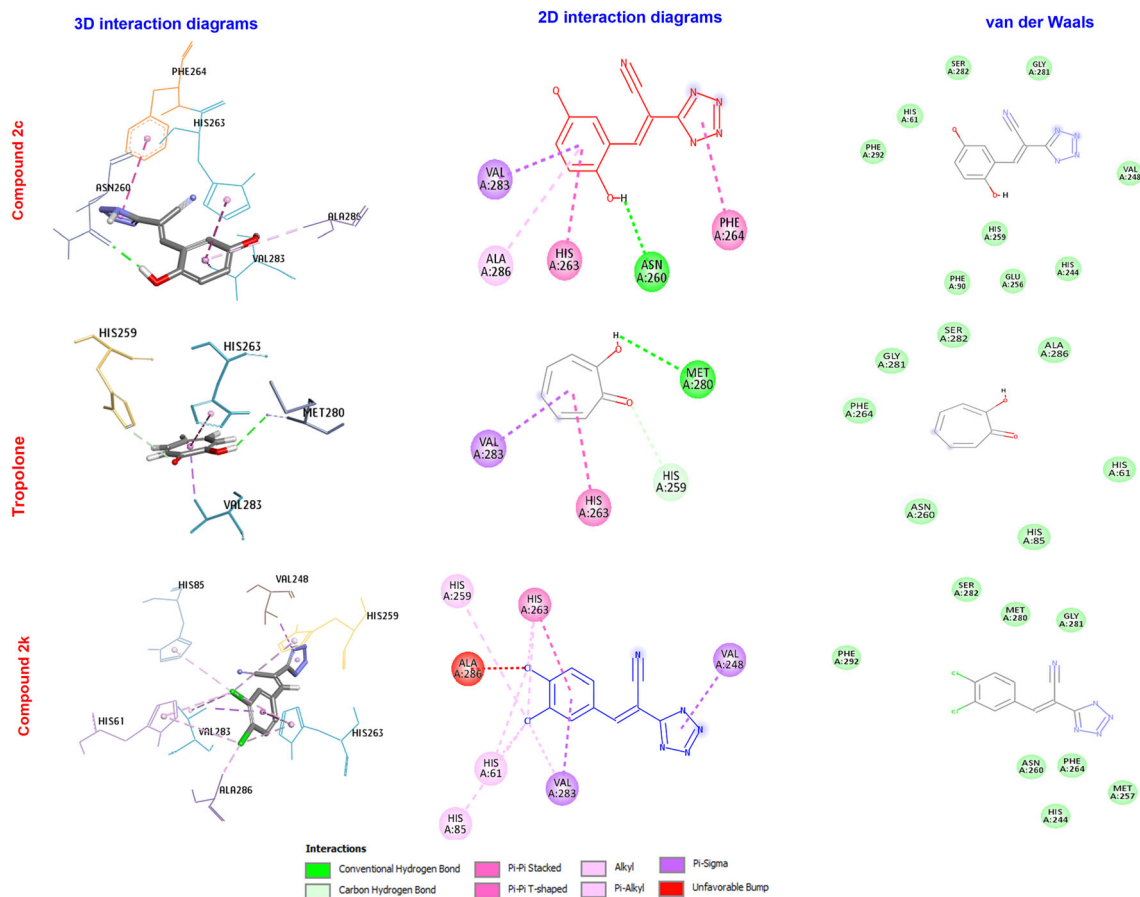
**Figure 5.** Protein-ligand interaction profiles of compounds 2c and 2k with tyrosinase and comparison of poses with reference ligand

The blood–brain barrier (BBB) is considered a physical barrier that protects the brain from the physical and biochemical flow.[41] It is important in terms of toxicity that molecules whose target is not the brain have not crossed this barrier. Bioavailability Radar is a graph that quickly shows drug similarity properties by calculating the physicochemical properties of molecules such as lipophilicity, size, polarity, solubility, flexibility, and saturation (Figure 3). The pink area shows the optimal range for each parameter. New molecules meet other physicochemical parameters other than saturation, as in the reference molecule. As can be seen in Table 4, the molecules conform to the Lipinski "Rule of Five." Cytochromes P450 show an important group of enzymes involved in the conversion of drugs in metabolism and rendering them harmless. Biotransformation of most of the drugs is carried out by five major isoforms (CYP1A2, CYP3A4, CYP2C19, CYP2C9, CYP2D6). Their inhibition may affect the elimination of other drugs, causing either toxic effects or undesirable side effects.[42] The inhibition potential of newly synthesized compounds against these isoforms is shown in

Table 4. Derivatives were scored as non-inhibitors of CYP isoforms, and only derivative 2c showed inhibition against CYP1A2.

## 4. Conclusions

In summary, PdAlO(OH) nanoparticles were used to synthesize 5-substituted-1H-tetrazole derivatives. Twelve derivatives were synthesized by the method developed under mild conditions. The tyrosinase enzyme activity of the synthesized derivatives was investigated. The results were compared with the reference molecule, tropolone. As a result of the studies, it was determined that the whole series synthesized had tyrosinase enzyme inhibition potential. In particular, the enzyme inhibitor potential of two compounds, compounds 2c and 2k, was quite high. In addition, molecular docking studies were performed to evaluate the binding and orientation of 2c and 2k compounds with high inhibitory activity to tyrosinase. As a result, it was determined that the related compounds interacted with specific amino acids and copper ions in the active site of the enzyme and that the factors causing

**Table 5.** Prediction of compound 2k, 2c, and tropolone ADME properties using SwissADME

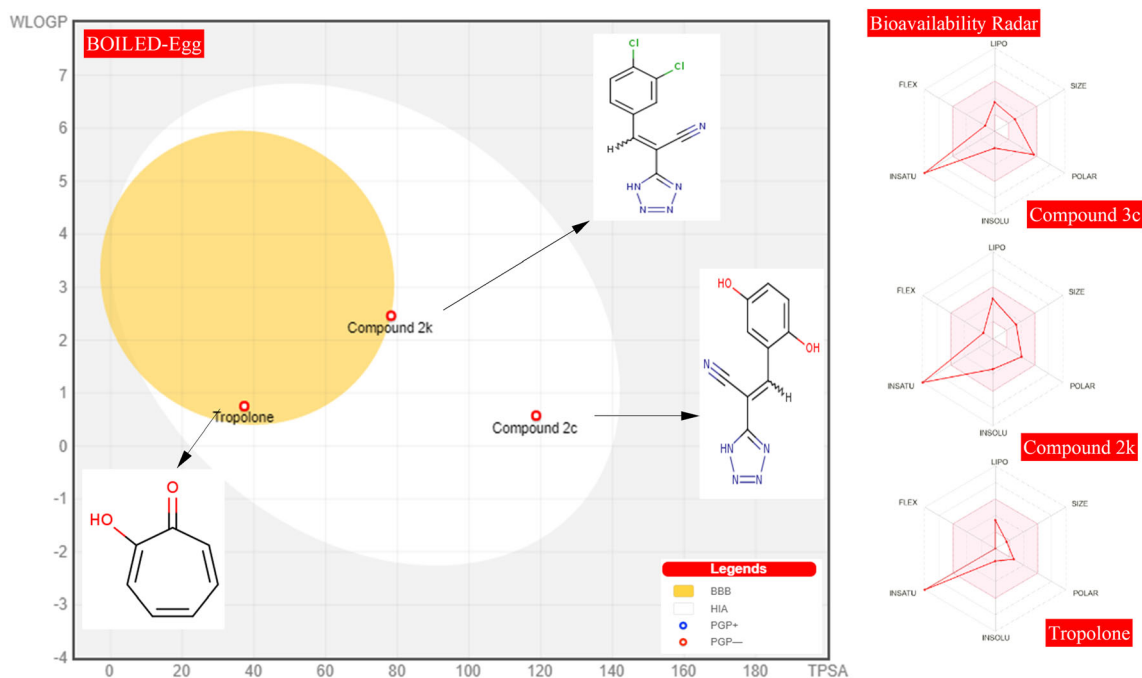| | Compound 2k | Compound 2c | Tropolone |
|---|---|---|---|
| Num. heavy atoms | 17 | 17 | 9 |
| Num. arom. heavy atoms | 11 | 11 | 7 |
| Fraction Csp3 | 0.00 | 0.00 | 0.00 |
| Num. rotatable bonds | 2 | 2 | 0 |
| Num. H-bond acceptors | 4 | 6 | 2 |
| Num. H-bond donors | 1 | 3 | 1 |
| Molar Refractivity | 64.12 | 58.15 | 34.74 |
| TPSA ($\text{Å}^2$) | 78.25 $\text{Å}^2$ | 118.71 $\text{Å}^2$ | 37.30 |
| Log $P_{o/w}$ (XLOGP3) | 2.62 | 0.65 | 0.53 |
| Log $S$ (ESOL) | -3.49 | -2.02 | -1.51 |
| Solubility | 8.67e-02 mg/mL; 3.26e-04 mol/l | 2.20e+00 mg/mL; 9.61e-03 mol/l | 3.80e+00 mg/mL; 3.11e-02 mol/l |
| Class | Soluble | Soluble | Very soluble |
| GI absorption | High | High | High |
| BBB permeant | No | No | Yes |
| P-gp substrate | No | No | No |
| CYP1A2 inhibitor | Yes | No | No |
| CYP2C19 inhibitor | No | No | No |
| CYP2C9 inhibitor | No | No | No |
| CYP2D6 inhibitor | No | No | No |
| CYP3A4 inhibitor | No | No | No |
| Log $K_p$ (skin permeation) | -6.06 cm/s | -7.24 cm/s | -6.67 cm/s |
| Lipinski | Accepted | Accepted | Accepted |

**Figure 6.**  BOILED-Egg models and the bioavailability radar graphs of compounds 2c, 2k, and tropolone using the SwissADME predictor

this affinity were some intermolecular interactions. The potential tyrosinase enzyme inhibitors of successfully synthesized tetrazole derivatives are a promising development for future studies.

## Supplementary Information (SI)

Supplementary material pertaining to this article is available at www.ias.ac.in/chemsci.

## References

1. Zarganes-Tzitzikas T, Chandgude A L and Dömling A 2015 Multicomponent reactions, union of MCRs and beyond *Chem. Rec.* **15** 981
2. (a) Neochoritis C G, Zhao T and Dömling A 2019 Tetrazoles via multicomponent reactions *Chem. Rev.* **119** 1970; (b) Herr R J 2002 5-Substituted-1H-tetrazoles as carboxylic acid isosteres: medicinal chemistry and synthetic methods *Bioorg. Med. Chem.* **10** 3379
3. Zou Y, Liu L, Liu J and Liu G 2020 Bioisosteres in drug discovery: focus on tetrazole *Fut. Med. Chem.* **12** 91
4. El-Barghouthi M I, Hasan A S, Al-Awaida W, Al-Ameer H J, Kaur J, Hayashibara K J, *et al.* 2022 Novel therapeutic heterocycles as selective cyclooxygenase-2 inhibitors and anti-cancer agents: Synthesis, in vitro bioassay screenings, and molecular docking studies *J. Mol. Struct.* **1263** 133141
5. (a) Oulous A, Daoudi N E, Harit T, Cherfi M, Bnouham M and Malek F 2022 New pyrazole-tetrazole hybrid compounds as potent α-amylase and non-enzymatic glycation inhibitors *Bioorg. Med. Chem. Lett.* **69** 128785; (b) Peng W, Liu F, Zhang L, Zhang L and Li J 2023 Design, synthesis, and evaluation of tricyclic compounds containing phenyl-tetrazole as XOR inhibitors *Eur. J. Med. Chem.* **246** 114947
6. Ni T, Chi X, Xie F, Li L, Wu H, Hao Y, *et al.* 2022 Design, synthesis, and evaluation of novel tetrazoles featuring isoxazole moiety as highly selective antifungal agents *Eur. J. Med. Chem.* **246** 115007
7. Labib M B, Fayez A M and EL-Shaymaa E N, Awadallah M and Halim P A 2020 Novel tetrazole-based selective COX-2 inhibitors: Design, synthesis, anti-inflammatory activity, evaluation of PGE2, TNF-α, IL-6 and histopathological study *Bioorg. Chem.* **104** 104308
8. Hajizadeh Z, Hassanzadeh-Afruzi F, Jelodar D F, Ahghari M R and Maleki A 2020 Cu(II) immobilized on $Fe_3O_4$@HNTs–tetrazole (CFHT) nanocomposite: synthesis, characterization, investigation of its catalytic role for the 1,3 dipolar cycloaddition reaction, and antibacterial activity *RSC Adv.* **10** 26467
9. Cardoso-Ortiz J, Leyva-Ramos S, Baines K M, Gómez-Durán C F A, Hernández-López H, Palacios-Can F J, Valcarcel-Gamiño J A, Leyva-Peralta M A and Razo-Hernández R S 2023 Novel ciprofloxacin and norfloxacin-tetrazole hybrids as potential antibacterial and antiviral agents: Targeting S. aureus topoisomerase and SARS-CoV-2-MPro *J. Mol. Struct.* **1274** 134507

10. Zhan P, Liu H, Liu X, Wang Y, Pannecouque C, Witvrouw M and De Clercq E 2010 Synthesis and anti-HIV activity evaluation of novel N′-arylidene-2-[1-(naphthalen-1-yl)-1H-tetrazol-5-ylthio]acetohydrazides *Med. Chem. Res.* **19** 652

11. Gao C, Chang L, Xu Z, Yan XF, Ding C, Zhao F, *et al.* 2019 Recent advances of tetrazole derivatives as potential anti-tubercular and anti-malarial agents *Eur. J. Med. Chem.* **163** 404

12. Zhang J, Wang S, Ba Y and Xu Z 2019 Tetrazole hybrids with potential anticancer activity *Eur. J. Med. Chem.* **178** 341

13. Maddila S, Naicker K, Momin M I, Rana S, Gorle S, Maddila S, *et al.* 2016 Novel 2-(1-(substitutedbenzyl)-1H-tetrazol-5-yl)-3-phenylacrylonitrile derivatives: synthesis, in vitro antitumor activity and computational studies *Med. Chem. Res.* **25** 283

14. Zakerzadeh E, Salehi R and Mahkam M 2017 Smart tetrazole-based antibacterial nanoparticles as multifunctional drug carriers for cancer combination therapy *Drug Dev. Ind. Pharm.* **43** 1963

15. Hasue K and Matsukawa M 2016 Mixtures of phase-stabilized ammonium nitrate containing 10 wt% potassium nitrate and tetrazoles as gas-generating agents *Sci. Technol. Energ. Mater.* **77** 98

16. Manzoor S, Yin X and Zhang J G 2021 Nitro-tetrazole based high performing explosives: Recent overview of synthesis and energetic properties *Def. Technol.* **17** 1995

17. Fischer N, Fischer D, Klapötke T M, Pierceya D G and Stierstorfera J 2012 Pushing the limits of energetic materials-the synthesis and characterization of dihydroxylammonium 5,5′-bistetrazole-1,1′-diolate *J. Mater. Chem.* **22** 20418

18. Mohammed J H 2016 Biological activities importance of Tetrazole derivatives *Eur. Acad. Res.* **3** 12796

19. (a) Salahshournia B, Hamadi H and Nobakht V 2018 Engineering a Cu-MOF nano-catalyst by using post-synthetic modification for the preparation of 5-substituted 1H-tetrazoles *Appl. Organomet. Chem.* **32** e4416; (b) Ghorbani-Choghamarani A, Moradi P and Tahmisi B 2016 Ni–S-methylisothiourea complexes supported on boehmite nanoparticles and their application in the synthesis of 5-substituted tetrazoles *RSC Adv.* **6** 56638

20. (a) Safaei-Ghomi J and Paymard-Samani S 2015 Facile and rapid synthesis of 5-substituted 1H-tetrazoles VIA a multicomponent domino reaction using nickel(II) oxide nanoparticles as catalyst *Chem. Heterocycl. Comp.* **50** 1567; (b) Akbarzadeh P, Koukabi N and Kolvari E 2019 Three-component solvent-free synthesis of 5-substituted-1H-tetrazoles catalyzed by unmodified nanomagnetite with microwave irradiation or conventional heating *Res. Chem. Intermediat.* **45** 1009

21. (a) Khodamorady M and Bahrami K 2019 Fe₃O₄@ BNPs-CPTMS-Chitosan-Pd(0) as an Efficient and Stable Heterogeneous Magnetic Nanocatalyst for the Chemoselective Oxidation of Alcohols and Homoselective Synthesis of 5-Subestituted 1H-Tetrazoles *ChemistrySelect* **4** 8183; (b) Mohammadi M, Khodamorady M, Tahmasbi B, Bahrami K and Ghorbani-Choghamarani A 2021 Synthesis of tetrazoles catalyzed by a new and recoverable nanocatalyst of cobalt on modified boehmite NPs with 1,3-bis(pyridin-3-yl-methyl)thiourea *J. Indust. Eng. Chem.* **97** 1

22. Samadi Garjaei S, Koukabi N and Nouri Parouch A 2022 Nano-Fe₃O₄/In: a heterogeneous magnetic nanocatalyst for synthesis of tetrazole derivatives under solvent-free conditions *Inorg. Nano-Metal Chem.* **52** 1050

23. Safaei-Ghomi J, Paymard-Samani S, Zahedi S and Shahbazi-Alavi H 2015 Sonochemical synthesis of 5-substituted 1H-tetrazoles catalyzed by ZrP₂O₇ nanoparticles and regioselective conversion into new 2,5-disubstituted tetrazoles *Z. Fur. Naturforsch.* **70** 819

24. Akbarzadeh P, Koukabi N and Hosseini M M 2020 Magnetic carbon nanotube as a highly stable and retrievable support for the heterogenization of sulfonic acid and its application in the synthesis of 2-(1H-tetrazole-5-yl) acrylonitrile derivatives *J. Heterocycl. Chem.* **57** 2455

25. Nouri Parouch A, Koukabi N and Abdous E 2020 Tetrazole derivatives synthesis using Fe₃O₄@fibroin-SO₃H as a magnetically separable green solid acid nanocatalyst under solvent-free conditions *Res. Chem. Intermed.* **46** 3295

26. Yuan X, Wang Z, Zhang Q and Luo J 2019 An intramolecular relay catalysis strategy for Knoevenagel condensation and 1,3-dipolar cycloaddition domino reactions *RSC Adv.* **9** 23614

27. Safapoor S, Dekamin M G, Akbari A and Naimi-Jamal M R 2022 Inflammasome NLRP3 activation induced by Convulxin, a C-type lectin-like isolated from *Crotalus durissus terrificus* snake venom *Sci. Rep.* **12** 1

28. Choi J, Choi K E, Park S J, Kim S Y and Jee J G 2016 Ensemble-based virtual screening led to the discovery of new classes of potent tyrosinase inhibitors *J. Chem. Inf. Model.* **56** 354

29. Qamar R, Saeed A, Larik F A, Abbas Q, Hassan M, Raza H and Seo S Y 2019 Novel 1,3-oxazine-tetrazole hybrids as mushroom tyrosinase inhibitors and free radical scavengers: Synthesis, kinetic mechanism, and molecular docking studies *Chem. Biol. Drug Des.* **93** 123

30. Yırtıcı U, Ergene A, Atalar M N and Adem S 2022 Phytochemical composition, antioxidant, enzyme inhibition, antimicrobial effects, and molecular docking studies of Centaurea sivasica *S. Afr. J. Bot.* **144** 58

31. Thomsen R and Christensen M H 2006 MolDock: a new technique for high-accuracy molecular docking *J. Med. Chem.* **49** 3315

32. Ismaya W T, Rozeboom H J, Weijn A, Mes J J, Fusetti F, Wichers H J and Dijkstra B W 2011 Crystal structure of Agaricus bisporus mushroom tyrosinase: identity of the tetramer subunits and interaction with tropolone *Biochem.* **50** 5477

33. DeLano W L 2002 PyMol: An Open-Source Molecular Graphics Tool *Protein Crystal.* **40** 82

34. Göksu H 2015 Recyclable aluminium oxy-hydroxide supported Pd nanoparticles for selective hydrogenation of nitro compounds via sodium borohydride hydrolysis *New J. Chem.* **39** 8498

35. Kahn V and Andrawis A 1985 Inhibition of mushroom tyrosinase by tropolone *Phytochem.* **24** 905

36. Otasek D, Morris J H, Bouças J, Pico A R and Demchak B 2019 Cytoscape automation: empowering workflow-based network analysis *Genome Biol.* **20** 1

37. Shihab I A, Muhammed M Y, Alheety M A, Nuaman H A and Karadag A 2023 Rapid ultrasound-assisted synthesis, characterization, DFT, molecular docking, and anticancer activity of palladium and zinc complexes with 2,6-dimethoxybenzoic acid: A comprehensive study *J. Mol. Struct.* **1294** 136259

38. Sarkar P, Alheety M A and Srivastava V 2023 Molecular docking and ADMET study of spice-derived potential phytochemicals against human DNA topoisomerase III alpha *Macromol. Symp.* **407** 2200108

39. Decker H, Schweikardt T and Tuczek F 2006 The first crystal structure of tyrosinase: all questions answered? *Angew. Chem. Int. Ed.* **45** 4546

40. Alheety M A, Jarullah A A, Mohammed M Y, Mahmood A R and Aydin A 2023 Pt phosphor-, oxygen-rich complexes: One pot synthesis, characterization, molecular docking and antiproliferative study *Inorg. Chim. Acta* **548** 121395

41. Daina A and Zoete V 2016 A boiled-egg to predict gastrointestinal absorption and brain penetration of small molecules *ChemMedChem* **11** 1117

42. Kirchmair J, Göller A H, Lang D, Kunze J, Testa B, Wilson I D, *et al.* 2015 Predicting drug metabolism: experiment and/or computation? *Nat. Rev. Drug. Discov.* **14** 387